

AirNet: Energy-Aware Deployment and Scheduling of Aerial Networks

Elif Bozkaya^{*†}, Klaus-Tycho Foerster[‡], Stefan Schmid[‡] and Berk Canberk[†]

^{*}Department of Computer Engineering, National Defense University Naval Academy, Istanbul, Turkey

[†]Department of Computer Engineering, Istanbul Technical University, Istanbul, Turkey

[‡]Faculty of Computer Science, University of Vienna, Austria

Email: bozkayae@itu.edu.tr, klaus-tycho.foerster@univie.ac.at, stefan_schmid@univie.ac.at, canberk@itu.edu.tr

Abstract—Aerial Base Stations (ABSs) promise resilient and perpetual connectivity after unexpected events such as disasters. However, the deployment and scheduling of ABSs introduce several algorithmic challenges. In particular, on-demand communication can change over time and be hard to accurately predict, so it needs to be handled in an online manner, accounting also for battery consumption constraints. This paper presents *AirNet*, an efficient software-based solution to operate ABSs by meeting these requirements. *AirNet* is based on an efficient placement algorithm for ABSs which maximizes the number of covered users, and a scheduler which navigates and recharges ABSs in an energy-aware manner. To this end, we formulate the problem of ABS deployment and propose an energy-aware deployment algorithm. In addition, we evaluate a novel scheduling mechanism that efficiently manages the ABSs’ operations. Our simulations indicate that our approach can improve connectivity and reduce energy costs significantly compared to a recent state-of-the-art approach.

Index Terms—Aerial Base Stations, energy efficiency, endurance, hover time, demand-aware deployment

I. INTRODUCTION

According to the Weather, Climate & Catastrophe Insight 2017 Annual Report [1], the direct economic damage of weather and climate topped USD353 billion dollars in 2017. Thus, over the last years, interesting novel technologies have emerged for disaster assistance, revolving around highly mobile and low-cost aerial platforms. The aim of such aerial platforms is to meet urgent communication needs in mission critical environments. Especially, the use of Aerial Base Stations (ABSs), e.g. drones, has become a prominent solution: when the existing terrestrial network is temporarily damaged, ABS-based wireless communications can provide adaptive coverage and high service quality for User Equipments (UEs) on the ground.

In addition, it is expected that nearly 12% of global mobile traffic will be 5G cellular connectivity by 2022, where an average 5G connection will generate 21GB of traffic per month [2]. Thus, the use of ABSs also assists to increase the coverage of the existing terrestrial networks.

The success of this technology rests on (i) energy efficient deployment and (ii) controlling ABSs’ operations in a co-ordinated manner. The ABS connectivity is built on top of the existing terrestrial wireless networks. Compared to conventional BSs, ABSs can adjust their position and provide on-demand communications to UEs. However, due to weight and

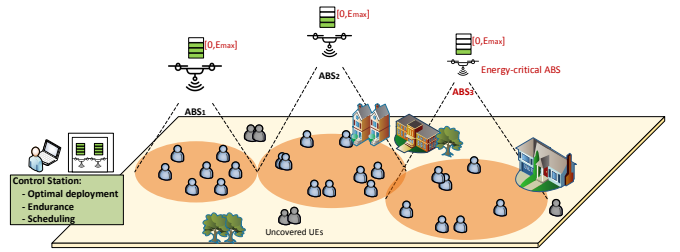


Fig. 1. Considered Scenario for Aerial Networks.

size constraints, ABSs have limited operational time before batteries have to be recharged. Their limited energy affects the network lifetime sacrificing throughput. While multiple ABSs are needed to ensure high service quality to the UEs, they introduce several algorithmic challenges, specifically in terms of energy-aware optimal deployment, endurance and scheduling. Defining the ABS positions is a key first step in network planning for long-lived Aerial Networks. Then, energy saving mechanisms and intelligent duty cycle can be managed by a control station.

In this paper, we focus on a practical scenario, where ABSs provide emergency coverage to the disaster area after terrestrial BSs are malfunction as shown in Fig. 1. We provide a continuous coverage model that aims to maximize hover time through an energy efficient deployment and reduces battery recharging time. The control station implements *optimal ABS deployment, maximizing endurance and scheduling for recharging* functionalities to manage ABSs. The control station identifies the optimal subset of UEs, via a deployment algorithm, to assign ABSs. After the placement of ABSs, the control station now tracks the consumed energy to specify the duration for which ABSs should be recharged. Thus, the key challenges in creating such a model are: (i) ensuring coverage model for ABSs from an online perspective, (ii) maximizing the flight endurance to serve UEs as long as possible and (iii) scheduling the operations of ABSs. Note that user demands can vary over time in unpredictable ways and satisfying these demands requires flexibility to reconfigure the network in an online manner. Thus, this paper explores the scenario where user demands are not entirely predictable and not known a priori.

More specifically, this paper presents *AirNet*, an energy

efficient software-based solution for ABSs that improves user coverage and flight endurance. More specifically, we make the following contributions:

- An energy-optimal placement algorithm is proposed to maximize covered UEs under limited battery capacity and limited number of ABSs. The demand-aware configuration is also analyzed from an online-manner perspective.
- We use an energy model to derive an efficient recharging strategy such that the total energy consumption for all ABSs is followed by taking into account affecting parameters including weight, flying time and flying speed.
- A scheduling mechanism is presented to assign ABSs to the limited number of replenishment stations, which can avoid ABSs to be out of service for a long time.
- We report on an extensive evaluation showing average 24% improvement in user coverage and 8% extension in the flight endurance compared to a recent state-of-the-art approach.

In order to facilitate future research and ensure reproducibility of our results, we will release our implementation and measured data publicly to the research community together with this paper.

The rest of the paper is organized as follows: We review related work in Section II. In Section III, we discuss the network architecture and model. In Section IV, we give the *AirNet* system. In Section V, we validate our model with extensive simulations and conclude the paper in Section VI.

II. RELATED WORK

The challenges related to the energy-efficient deployment [12]-[13] and optimization of endurance [14]-[15] for Aerial Networks have already been intensively studied in the literature. We will review related works in these areas in turn and put the novelty of our contribution into perspective in the following.

Coverage Problem and ABS Deployment: In [8], the authors address multiple cooperative coverage problems for more reliable and efficient aerial scenarios and propose a multi-UAV coverage model based on energy-efficient communication. First, the coverage probability from a given UAV is derived. Then, transmission power is determined to maximize coverage utility. Although the locations of users are known a priori, the user demands cannot be entirely predictable and this affects the coverage model. In [9], the authors focus on maximizing the coverage area of a single ABS under the constraint of transmission power. Then, the relationship between antenna gain and antenna beam angle is set up so that flight altitude and coverage radius are adjusted according to beam angle. However, the provided solution cannot be optimal with multiple ABSs. In [11], the authors propose a deployment algorithm for UAV-BSs that maximizes the number of covered users with minimum transmission power. In horizontal dimension, deployment problem is modeled as circle placement problem and the results are confirmed with different user heterogeneity. However, the proposed solution are designed for 2D space. In [18], analysis and optimization of air-to-ground systems are researched. The authors derive optimal UAV altitude for reliable communication and maximum coverage area. However,

for reliable communication in Aerial Networks, energy is also an important factor that needs to be included in a working system.

Maximizing Flight Endurance: Due to the battery constraints of ABSs, many research projects aim to minimize the duration of ABS in reaching their designated locations so that hover time is maximized to achieve assigned tasks. In [10], the authors deal with the deployment problem to transport UAVs in the shortest time. In addition, the computational complexity is analyzed and an optimal solution is proposed. However, their problem is simplified by only focusing on predetermined clusters so that coverage area adjustment is not considered. In [16], survivability of the battery-operated aerial-terrestrial communication links is investigated to improve energy efficiency. However, Aerial Networks are constructed in the center of the target area so that it cannot be practical to maximize coverage area. In [17], throughput coverage is investigated by optimally placing UAVs for public safety communication after a natural disaster. In contrast, the consumed energy of ABSs in our work is investigated and endurance is improved. In [19], flight time constraints of ABSs and relationship between the hover time of ABSs and bandwidth efficiency are investigated. First, given the maximum possible hover time, average data service is maximized. Then, given the load requirements of users, average hover time of ABSs is minimized to completely serve the users. The key difference between [19] and our work is that we schedule the operations of ABSs' to improve the flight duration and serve the users as much as possible. In addition, we also jointly consider transition and hover time which both of them contribute to maximize endurance.

Path planning also provides some mechanisms to guarantee safe navigation of drones while avoiding collisions. In particular, with the usage area of drones in a wide range of applications, e.g., search and rescue operations, packet delivery service, traffic monitoring, drones can only achieve their missions by continuously updating the target region [30]. In order to maximize the collected data and reach the destination, path planning algorithms determine a path between source and destination node pairs. These algorithms include genetic algorithms [31], particle swarm optimization [32] or building a probability map [33] etc. The transition to the designated locations may face several uncertainties according to different path planning algorithms, such as obstacles, high computational complexity and unpredictability. This topic is not addressed in this paper. The main idea is to direct the ABSs to the designated location along a flight path by minimizing the travel length.

In terms of the underlying algorithmic problems, the coverage problem in Aerial Networks is related to problems such as the set cover and sweep coverage problems. For example, the *Set Cover Problem* looks for the fewest sets to cover a given set of points in the plane, which is NP-hard [24]. Our optimization problem can be seen as a geometric version, where the set size also depends on the height of the ABS [21]. Another related optimization problem considers a scenario, where a mobile drone/autonomous robot can continuously move to collect data from targets. By doing this, the robots aim to minimize so called sweep period for the given targets or reduce

the trajectory length. This problem is referred as the *Sweep Coverage Problem* [25]. In both problems, the objectives are to improve coverage utility and endurance (flight time) by maximizing energy efficiency. Following similar objectives, but considering a more general model, in this paper, we study the control of ABSs' operations with a centralized controller and find an energy-aware 3D deployment for ABSs by proposing a scheduling mechanism to maximize flight endurance. In this paper, we provide useful guidelines for controlling ABSs' operations.

III. NETWORK ARCHITECTURE AND MODEL

A. Network Model

We consider a square area of size $A \text{ m}^2$ ($a(m) \times a(m)$) and a set of M ABSs to cover the target area. Each ABS communicates with a number of UEs, which are uniformly distributed (UEs per m^2). An ABS recharges its battery at the replenishment station that is located on a mobile control station as depicted in Fig. 1. The control station executes the *Optimal ABS Deployment, Maximizing Endurance and Scheduling for Recharging* algorithms to manage the topology that will be detailed in the next section.

Each ABS can be in one of the following states as shown in Fig. 2(a). In addition, an ABS life cycle is shown in Fig. 2(b).

- Transiting State (s_{trans}): After the determination of the ABS locations, the consumed energy from the initial location to the designated location and also from the designated location to the initial location are followed in this state. For mathematical denotation, we refer to the transition times as $t_0 - t_1$ and $t_2 - t_3$, respectively.
- Hovering State (s_{hover}): In this state, UEs remain connected with ABSs and get service. We denote the hover time as $t_1 - t_2$.
- Recharging State ($s_{recharge}$): The ABS is on the replenishment station to recharge its battery.
- Sleeping State (s_{sleep}): If all replenishment stations are used by other ABSs, and thus there is no available station to recharge, ABSs are waiting in this state. In addition, if the available ABSs in the target area cover all UEs, the remaining ABSs are in this state until a new task is assigned by the control station.

In addition, we assume that each ABS starts with a maximum and identical energy capacity, equal to E_{max} , where the coverage utility depends on the energy available at the ABS on hovering state. More specifically, consumed energy between initial location $(0, 0, 0)$ to designated location (x_j, y_j, z_j) (transiting state) will directly affect the lifetime of the ABS. The parameters used in the paper are described in Table I.

Considering joint ABSs' coverage, the coverage probability of an UE_{*i*} is [3]:

$$\begin{aligned} P_{cov,i} &= \mathbb{P}\left[\frac{P_{r,i}}{N + I} \geq P_{threshold}\right] \\ &= P(LoS)_i \mathbb{P}[P_{r,i}(LoS) \geq P_{min}] + \\ &\quad P(NLoS)_i \mathbb{P}[P_{r,i}(NLoS) \geq P_{min}] \end{aligned} \quad (1)$$

where P_{min} is the minimum received power, $P_{min} = 10 \log(NP_{threshold} + IP_{threshold})$, N is the noise power. We

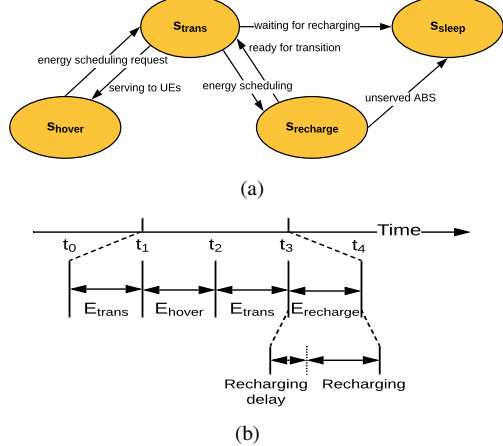


Fig. 2. (a) Energy efficient states for ABSs (b) ABS life cycle.

TABLE I
PARAMETERS

Parameter	Description
M	Number of ABSs
A	The size of target area (Please note that a is the length of one side of the square)
$P_{cov,i}$	Coverage probability of UE _{<i>i</i>}
P_t	Transmission power of ABS
$P_{r,i}$	Received power by UE _{<i>i</i>}
P_{min}	Minimum received power
E_{max}	ABS battery capacity
N	Noise power
I	Interference received from the nearest ABS
$P(LoS)$	LoS probability
$P(NLoS)$	NLoS probability
$P_{threshold}$	SNIR threshold ratio
η	Path loss coefficient
$g(\varphi_k)$	Antenna gain
θ	Elevation angle
f_c	Carrier frequency
n	Path loss coefficient
ρ	Air density
m_d	ABS weight
m	ABS propeller
v_d	Average ABS speed
v_{max}	Maximum ABS speed

assume that noise power does not change over time for all receivers for simplicity and is equal to -120 dBm . $P_{threshold}$ is the Signal-to-Interference and Noise (SINR) threshold ratio. This shows the necessary condition for connecting the UEs to ABSs and I is the interference power received from the nearest ABS k [3]:

$$I \approx P_t g(\varphi_k) \left[10^{-\frac{\mu_{LoS}}{10}} P_{LoS,k} + 10^{-\frac{\mu_{NLoS}}{10}} P_{NLoS,k} \right] \left(\frac{4\pi f_c d_k}{c} \right)^{-n} \quad (2)$$

where P_t is the transmission power of ABS, $g(\varphi_k)$ is antenna gain, where $\approx 29000/\theta^2$ [3] and θ is elevation angle, f_c is the carrier frequency, c is the speed of light. μ_{LoS} and μ_{NLoS} are the mean of the shadow fading for LoS and NLoS and n is the path loss exponent ($n = 2$).

The received signal from ABS for UE_{*i*} is as follows [4]-[5]:

$$P_{r,i}(\text{dB}) = \begin{cases} P_t + g - PL_{LoS,i} - \chi_{LoS}, & \text{for LoS link} \\ P_t + g - PL_{NLoS,i} - \chi_{NLoS}, & \text{for NLoS link} \end{cases} \quad (3)$$

where $\chi_{LoS} \sim N(\mu_{LoS}, \sigma_{LoS}^2)$ and $\chi_{NLoS} \sim N(\mu_{NLoS}, \sigma_{NLoS}^2)$ are the impact of shadowing caused by obstacles with normal distribution. $(\mu_{LoS}, \sigma_{LoS}^2)$ and $(\mu_{NLoS}, \sigma_{NLoS}^2)$ are mean and variance of shadow fading for LoS and NLoS where $\sigma_{LoS}(\theta_j) = k_1 \exp(-k_2 \theta_j)$ and $\sigma_{NLoS}(\theta_j) = g_1 \exp(-g_2 \theta_j)$, respectively [3]-[29]. The values of k_1, k_2, g_1, g_2 depend on the environment and constant. PL_i is the path loss. We use the path loss model for air-to ground communication over urban environments. Each UE will have a LoS and NLoS links with some probability by connecting to the ABS. This probabilities depend on the location of UE and ABS, and environment. The LoS probability between the ABS and UE is given by [4], [5]:

$$P(LoS)_i = \frac{1}{1 + a \cdot \exp(-b[\theta - a])} \quad (4)$$

where a and b are constant values that depend on the type of the environment (rural, urban etc). θ is the elevation angle and equal to $\theta = \frac{180}{\pi} \arctan(\frac{h}{d_i})$. h and d_i represent the altitude of the ABS and distance between the ABS and UE _{i} . Note that the NLoS probability between UE and ABS is equal to $P(NLoS_i) = 1 - P(LoS_i)$.

Then, the path loss model for LoS and NLoS is given by [4]-[5]:

$$PL_i(dB) = \begin{cases} 20 \log \left(\frac{4\pi f_c d_i}{c} \right) + \eta_{LoS}, & \text{for LoS link} \\ 20 \log \left(\frac{4\pi f_c d_i}{c} \right) + \eta_{NLoS}, & \text{for NLoS link} \end{cases} \quad (5)$$

where η_{LoS} and η_{NLoS} are additional path loss coefficient and f_c is 2GHz with η_{LoS} and η_{NLoS} is equal to 1 and 20, respectively for urban environments [29].

B. Architectural Model

Fig. 3 shows the implementation of the control architecture. An ABS is equipped with a RF receiver to receive control signals sent by a control station.

A task is defined by the control station for each ABS that will be executed. For a first scenario, the ABS follows its fixed task and no external communication is required. However, the defined task can be updated by the control station based on the network architecture. The *set up* block provides flight control information including hover location, coverage area, flight route and speed. The *critical controller* only includes critical control functionality to provide an indication for energy consumption based on defined time units. In every time unit, control decisions are computed by the control station, and commands are sent to the ABSs. Once the consumed energy is known, the remaining energy information is evaluated with the distance between the control station and ABS so that timely and adaptive control decisions works in software. For this purpose, the *dynamics* block stabilizes the ABS. Rather than periodically triggering the controller of ABSs, we only run the

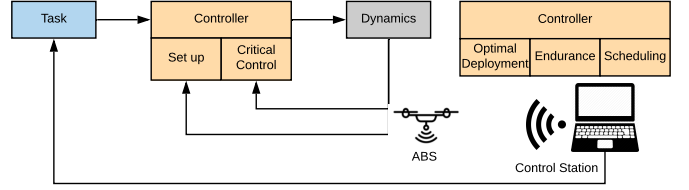


Fig. 3. Control Architecture.

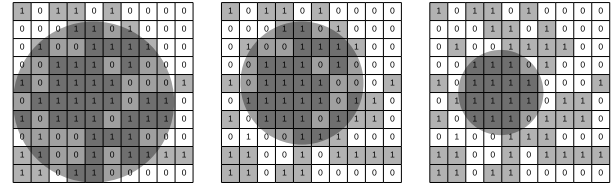


Fig. 4. Adjustment of coverage area with a single ABS.

set up block when an update is needed and the critical control is checked when an critical energy threshold is reached.

IV. AirNet SYSTEM

In this section, we provide an energy-aware solution, *AirNet* to deploy and schedule ABSs and maximize hover time with an endurance framework. We will describe *AirNet* in multiple steps.

A. Optimal ABS Deployment

To simplify the presentation, we first analyze the single ABS deployment to cover the target area. In Fig. 4, the target area is divided into grid cells ($Cx Cm^2$). Each cell is marked as '1', which means that this area includes a number of UEs. Here, the number of UEs can vary from cell to cell. Our main idea for this demonstration is to observe the density of the UEs in the target area. Otherwise, it is marked as '0' to show the empty cell state. This means that there is no UEs in this cell. An example illustration is shown in Fig.4. Depending on the altitude of the ABS, the coverage area also changes. Here, we define $R_{cluster}$ so that UE cannot be connected to the ABS out of this area. At the initial phase, according to UE locations, we find the center of minimum radius to cover maximum number of UEs. Mathematically, with the *Chebyshev Center* formulation, the problem can be written as follows:

$$\min_{\mathbf{x}, R_{cluster}} R_{cluster} \quad (6)$$

subject to

$$\|\mathbf{x} - UE_i \leq R_{cluster}\|, \quad i = 1, 2, \dots, U. \quad (7)$$

where \mathbf{x} is the center point of the cluster and U is the number of UEs.

However, it may not be effective when the whole target area is only covered by one ABS because of the given transmission power and the flight altitude, where each UE cannot have a good signal quality. Therefore, we first define $R_{cluster}$ with h_{max} and then check the received power of UEs with the SINR threshold value as given in Eq. 1. At each step,

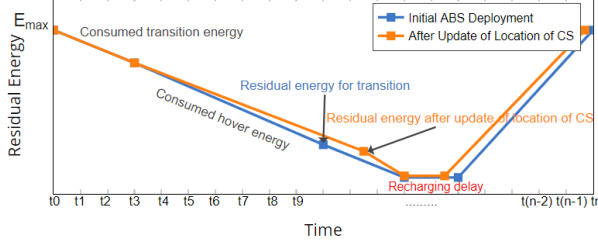


Fig. 5. Residual energy for two different cases.

we repeat this process with $h^* = (h_{min} + h_{max})/2$ until the solution is feasible. Then, we update the coverage area radius with Alg. 1 as shown in Fig. 4. Optimal ABS altitude enables maximum coverage area with a minimum required transmission power. Alg. 1 optimally solves the deployment problem with computational complexity of $O(n \log n)$. The analysis is performed for each ABS. We first note that h^* produced by Alg. 1 is feasible. Otherwise, Alg. 1 ends when $\left[\frac{P_{r,i}}{N+I} \geq P_{threshold} \right]$ for each $UE_i \in R_{cluster}$. Since we adjust the altitude between h_{min} and h_{max} for each ABS, we start with a maximum altitude to cover as possible as UE. Suppose we have our solution $x = (x_1, x_2, \dots, x_m)$, $y = (y_1, y_2, \dots, y_m)$ with optimal altitude $h = (h_1, h_2, \dots, h_m)$. U UEs are covered by one ABS. With the defined $R_{cluster}$ as given in Eq. 6, Line 2 is checked for $\forall UE_i \in R_{j,cluster}$. This is repeated for each deployed ABS. Please note that ABSs are directed along a flight path by minimizing the travel length.

Algorithm 1 Optimal ABS Deployment

- 1: Given : $h_{min} \leq h^*$, $h_{max} \geq h^*$
- 2: Tolerance : $\left[\frac{P_{r,i}}{N+I} \geq P_{threshold} \right]$
- 3: **repeat**
- 4: (1) $h^* = (h_{min} + h_{max})/2$
- 5: Solve the feasibility problem (1)
- 6: **if** (1) is feasible **then** $h_{max} = h^*$
- 7: **else** $h_{min} = h^*$
- 8: **until** $\forall UE_i \in R_{cluster} \left[\frac{P_{r,i}}{N+I} \geq P_{threshold} \right]$

With M ABSs and N UEs, the relationship can be represented as $a \in \mathbb{A}^{M \times N}$, where $a_{ij} = 1$ if UE_i is covered by ABS_j , otherwise $a_{ij} = 0$. Also we define a cost parameter, which is the consumed transition energy from the initial position (control station) to the designated position for ABSs. The consumed transition energy is given in Eq. 8 [6]-[7]:

$$E_{trans} = \left(\frac{P_{full} - P_s}{v_{max}} v_d + P_s \right) t_1 \quad (8)$$

where v_d is the average constant ABS speed during the trip, v_{max} is the maximum speed of the ABS and $t_1 = d/v_d$, d is the flying distance with a constant velocity. P_{full} is the hardware power levels when ABS is moving at full speed and P_s is the power levels when drone stops in a fixed position ($v_d = 0$). Therefore, the optimization problem minimizes

the cost for all ABSs to decrease the transition energy while covering maximum number of UEs as given in Eq. 9.

$$\min \sum_{j=1}^M \left[\left(\frac{P_{full} - P_s}{v_{max}} v_d + P_s \right) (t_3 - t_2) \right] x_j \quad (9)$$

subject to

$$C_1 : \sum_{j=1}^M a_{ij} x_j \geq 1 \quad (10)$$

$$C_2 : x_j \in \{0, 1\} \quad j \in M \quad (11)$$

where C_1 enables to select all UEs that are covered by ABS_j and x_j is a binary variable to follow active ABSs. As seen in Eq. 8, the consumed energy will increase with distance so that after the deployment of ABS, we focus on decreasing transition energy. To do this, we propose to update the location of the control station while guaranteeing the minimization of cost with Alg. 2. We illustrate the residual energy level with the updating procedure in Fig. 5. Here, we also aim to cover as much as possible UEs when the number of ABSs is limited. While the maximum coverage problem is NP-hard under the limited ABS (Line 2-5), we can obtain a greedy approximation factor of $1 - \frac{1}{e}$, which is explained in Appendix A [34].

Algorithm 2 Minimization of Cost

- 1: Initialize: $E_{trans,j} \leftarrow \emptyset$ and $U \leftarrow X$ (U is the set of uncovered UEs and X is the finite set of UEs)
 - 2: **while** $\forall ABS_j$ is deployed **do**
 - 3: Let S be a set such that $|S \cap U|$ is maximized (S covers the largest number of UEs in U)
 - 4: $U \leftarrow U \setminus S$ (remove from UEs in U that are covered by ABS_j)
 - 5: **end while**
 - 6: *DemandAwareReconfiguration()* // cf Section IV.B
 - 7: Update (x, y) position of MCS as $(x, y) = \frac{S_{1,x,y}, \dots, S_{M,x,y}}{M}$ ($S_{1,x,y}$ is the center point of set S_1)
 - 8: **for** $j \leftarrow 1$ to M **do**
 - 9: Calculate $E_{trans,j}$ with Eq. 8
 - 10: **end for**
 - 11: **return** $E_{trans,j}$
-

While a detailed evaluation is given in the next section, to get some intuition on the effectiveness of the algorithms, we conduct simple experiments first. This is performed in MATLAB, with an environment with single and 2 ABSs, respectively. Then, the commands are tested with MAVProxy 1.5.0 that runs on SITL (Software In The Loop) ArduPilot simulator using Cygwin [20]. We observe the coverage areas for better understanding of the performance of the network. Fig. 6 shows the deployment of a single ABS with $(10^{-4} UEs/m^2)$ and two ABSs with $(2 \times 10^{-4} UEs/m^2)$, respectively.

With different UE densities, we show the relationship between coverage radius, $R_{cluster}$ and optimal altitude in Fig. 7(a). Clearly, after the optimal height is obtained, as the height of ABS increases, the coverage radius will decrease because of the SINR. Under the SINR connection model, the altitude is adjusted between $h_{min} = 20m$ and $h_{max} = 100m$

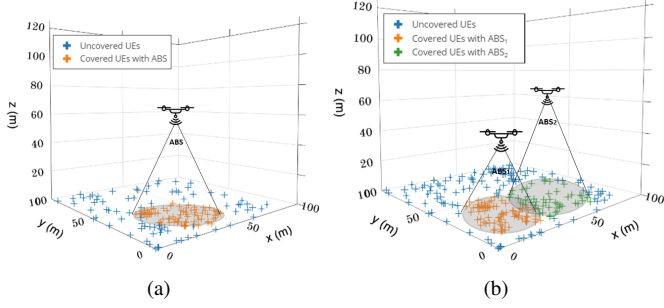


Fig. 6. (a) Coverage area with single ABS (10^{-4}UEs/m^2) (b) Coverage areas with 2 ABSs ($2 \times 10^{-4} \text{UEs/m}^2$).

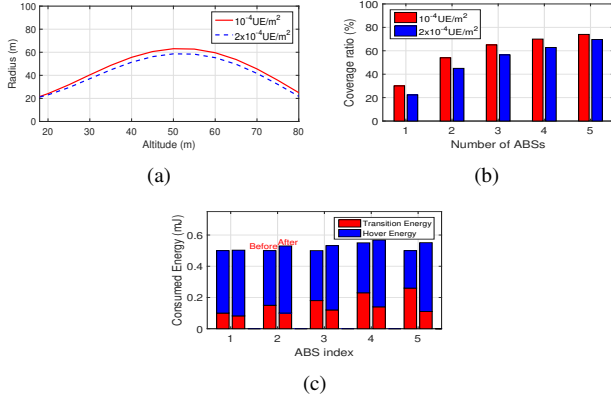


Fig. 7. (a) The relationship between coverage radius, $R_{cluster}$ and altitude (b) Coverage ratio with increasing number of ABSs (c) Consumed transition and hover energy before the first ABS deployment and after the update of location of control station.

to determine the strength of the received signal from the desired ABS and avoid interference caused by other ABS and the noise power. We also illustrate the coverage ratio with increasing number of ABSs for (10^{-4}UEs/m^2) and ($2 \times 10^{-4} \text{UEs/m}^2$) densities in Fig. 7(b). Then, we compare two different scenarios in Fig. 7(c) with 5 ABSs. At first, we deploy ABSs and calculate consumed transition and hover energy with Eqs. 8 and 21, respectively. Then, we update the location of control station as explained in Alg. 2 and obtain a degradation 14% in terms of consumed transition energy. This will enable to increase hover time of ABSs.

B. Demand-Aware Reconfiguration

One of the key features of *AirNet* is that it naturally supports demand-aware operation. User demand can vary over time in an unpredictable way, which leads us to analyze time-varying user demand. Satisfying the dynamic user demand requires reconfiguration in an online manner. Here, the novelty is a scenario that demands on the network are not entirely predictable and also not known a priori. Thus, an interesting question is how we can maintain quality of service.

To achieve this, we check the traffic load of ABSs for demand-aware reconfiguration. Here, we only focus on overlapping areas since coverage areas and the position of ABSs can be reconfigured to satisfy users' demands. Overlapping areas are the regions where UEs can connect k -ABS since

this region is covered by k -ABS. Therefore, we assign the UEs in the overlapping areas to the ABS which has low traffic load and accordingly, we change coverage area based on load balancing by adapting the altitude of ABSs.

Traffic demands are kept in a Demand Matrix in each time t_y , where $t_1 < t_y < t_2$ and represented as $|M \times N|_{t_y}$. An entry $D_{(i,j)}$ in D is the demand from UE _{i} to ABS _{j} , where each of variable packet size, L_i with power law distribution and their arrival rate, λ_i with Poisson distribution. Since user demand can vary with different types of applications, there should be a fair resource allocation among traffic demands to satisfy users' QoS. Here, we consider the well-known D'Hondt Algorithm [26]-[27] (seat allocation) to assign Resource Blocks (RB) to UEs. We initially assign minimum number of RBs to each UE. Then, if there are still unallocated RBs, we dynamically set the minimum number of RBs. Firstly, we set it too high, and then iteratively reduce until we reach the right value. At each stage, a RB is given to the UE with the highest demand, $T = \frac{\sum_{i=1}^N D_{ij,t_y}}{R_{t_y} + 1}$ and its value of R goes up by one where $\sum_{i=1}^N D_{ij,t_y}$ is the total number of demands at time t_y , R_{t_y} is the total number of resource blocks it has already been allocated.

C. Endurance Framework

Energy consumption of ABSs is of paramount importance for Aerial Networks since it directly affects the endurance and limits network lifetime. In general, the consumed energy by one ABS is (i) transition power, P_{trans} , from initial location to designated location, (ii) hover power, P_{hov} , to serve UEs and (iii) communication power, P_{com} , with control station. Minimizing each of them can help to extend ABSs' lifetime.

For this purpose, each ABS independently maximizes the endurance (Υ), which means the flight duration on hovering state of an ABS so that a higher hover energy a higher endurance. The problem can be considered as follows:

$$\Upsilon = \frac{E_{total} - [E_{trans,t_0-t_1} + E_{trans,t_2-t_3}]}{P_{hov}} \quad (12)$$

Accordingly, the optimization problem is to maximize the endurance as given in Eq. 13.

$$\max_{h_{min} \leq h^* \leq h_{max}, R_{cluster}} \Upsilon_j \quad \forall j \in M \quad (13)$$

subject to

$$C_1 : E_{res,t_y} \geq \int_{t_2}^{t_3} P_{trans} dt \quad (14)$$

$$C_2 : \theta_n \in [\theta_{min} - \theta_{max}] \quad (15)$$

$$C_3 : a_{ij,t_y} \in \{0, 1\} \quad (1 \leq i \leq N), (1 \leq j \leq M), (t_1 \leq t_y \leq t_2) \quad (16)$$

$$C_4 : \sum_{i=1}^N a_{ij,t} \leq 1 \quad (17)$$

where C_1 is the residual energy constraint, where will be detailed below. C_2 limits the relation between the altitude and coverage radius, where θ is the angle formed by the center of one of the circles and the points of intersection of the

circles. C_3 states that $a_{ij,t_y} = 1$, if ABS is serving UE in the designated time slot t_y , and otherwise $a_{ij,t_y} = 0$. Additionally, C_4 states that UE cannot serve more than one ABS in the designated time slot.

Total energy capacity of an ABS is given in Eq. 18:

$$E_{total} = \int_{t_0}^{t_1} P_{trans} dt + \int_{t_1}^{t_2} [P_{hov} + P_{com}] dt + \int_{t_2}^{t_3} P_{trans} dt \quad (18)$$

Accordingly, the hover power is given in Eq. 19:

$$P_{hov} = \frac{F^{3/2}}{\sqrt{2\rho A}} \quad (19)$$

where $F = m_d g$, m_d is the ABS weight (kg), g is the earth gravity (m/s^2), and $A = \pi r^2 m$, r is the radius of ABS's propellers and m is the number of drone's propellers. ρ is the air density (kg/m^3).

$$P_{hov} = \frac{(m_d g)^{3/2}}{\sqrt{2\pi r^2 m \rho}} \quad (20)$$

and

$$E_{hov} = \int_{t_1}^{t_2} \frac{(m_d g)^{3/2}}{\sqrt{2\pi r^2 m \rho}} dt \quad (21)$$

Transition energy is given in Eq. 8. On the other hand, the power consumption for the communication (P_{com}) is neglected to reduce the computation complexity.

E_{res,t_y} is the residual energy level of the ABS at time t_y and E_{con,t_y} is the consumed energy at time t_y where $t_1 < t_y < t_2$.

$$E_{res,t_y} = E_{max} - E_{con,t_y} \quad (22)$$

and

$$E_{con,t_y} = \int_{t_0}^{t_1} P_{trans} dt + \int_{t_1}^{t_y} P_{hov} dt \quad (23)$$

$$E_{res,t_y} \geq \int_{t_2}^{t_3} P_{trans} dt \quad (24)$$

In order to manage ABSs, we introduce Alg. 3. The principle is to track the residual energy of ABSs in each time slot and give a decision to recharge. After the recharging decision, we also calculate the consumed energy as given in Eq. 23 so that a lower the consumed energy, a quicker the charging time. Then, each ABS is either assigned to one of the replenishment station or programmed to the sleeping state. Each ABS needs to execute Line 2 and 3 of Alg. 3 per discrete time slot and take $O(1)$ operations. Similarly, Lines 4-7 are $O(1)$. Thus, total complexity is $O(n)$ operations per discrete time.

D. Scheduling between ABSs and Replenishment Stations

In Eq. 24, the controller follows the residual energy after the ABS is on hover and accordingly, gives a decision for the charging based on the threshold energy level. Please note that threshold energy level is different for each ABS and calculated in Alg. 3. The problem occurs if the number of ABSs that needs to be recharged is more than number of available replenishment stations at a time. Therefore, there is need a mechanism in order to prevent the out of service of these ABSs. If the ABSs that need to be recharged are not

Algorithm 3 Maximizing Endurance

```

1: for  $j \leftarrow 1$  to  $M$  do
2:    $E_{res,t_{y+1}} \leftarrow compute \forall j \in M$ 
3:    $E_{threshold} \leftarrow \int_{t_2}^{t_3} P_{trans}(t) //$ Please note that the location of control station is updated in Alg. 2
4:   if  $E_{res,t_{y+1}} < E_{threshold}$  then
5:     Schedule for charging
6:      $w_j \leftarrow E_{con,t_y}$ 
7:   end if
8: end for
9: Sort ABS according to  $w_j$  in ascending order
10: Select the ABSs in order for recharging

```

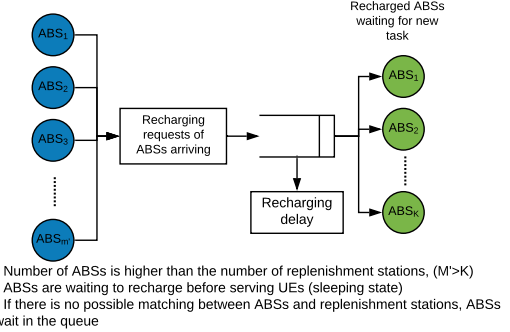


Fig. 8. Recharging requests of ABSs.

scheduled due to the less number of replenishment stations, these ABSs will be waited in the sleeping state to recharge as illustrated in Fig. 8. Thus, in the proposed model, the controller presents a recharging strategy and accordingly, schedules the ABS deployment.

With the proposed approach, the control station begins to manage replenishment stations with the first arrival of ABS and then update the system when a new arrival or departure occurs with Eqs. 25-26.

$$L = \sum_{n=1}^T x(t_n - t_{n-1})/T \quad (25)$$

and

$$W = \sum_{t_a, t_d \in T} [t_d - t_a]/M' \quad (26)$$

where L and W are mean number of the ABSs and mean charging time (min) in the replenishment station. x and M' represent the number of ABSs at time t and total number of arrival over the time period $[0, T]$. t_a and t_d are arrival and departure time of the ABSs in the system. This also shows the charging time of an ABS, where $[t_d - t_a] (min) = CE_{con}/I_c E_{max}$, C (in mAh) is the capacity of the battery and I_c (in Ampere) is the current of the charge.

For example, consider the illustration in Fig. 9(a), the number of the ABSs that arrives to the station for recharging over the time period $[0, T]$ is $M' = 4$. Black circles show the arrivals and red circles show the departures. L and W parameters are given in Eqs. 27-28 [22].

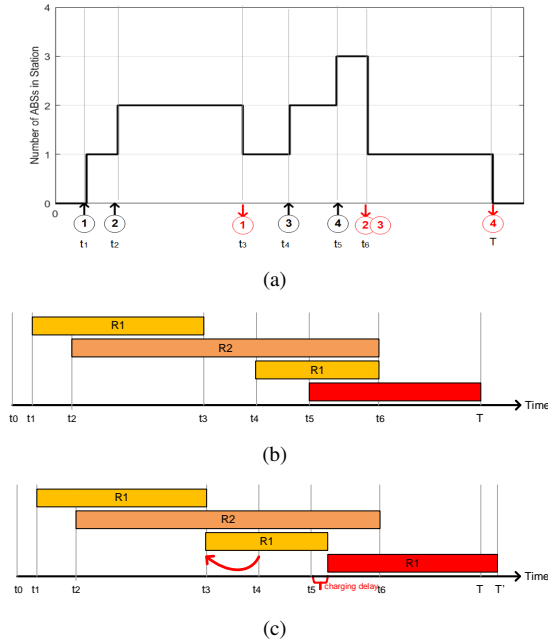


Fig. 9. (a) Illustration of busy period of replenishment station (b) Before scheduling (c) After scheduling.

$$\begin{aligned} L &= [1(t_2 - t_1) + 2(t_3 - t_2) + 1(t_4 - t_3) + 2(t_5 - t_4) \\ &\quad + 3(t_6 - t_5) + 1(T - t_6)]/T \\ &= [T + 2t_6 - t_5 - t_4 + t_3 - t_2 - t_1]/T \end{aligned} \quad (27)$$

$$\begin{aligned} W &= [(t_3 - t_1) + (t_6 - t_2) + (t_6 - t_4) + (T - t_5)]/K \\ &= [T + 2t_6 - t_5 - t_4 + t_3 - t_2 - t_1]/4 \end{aligned} \quad (28)$$

However, if we assume that the number of replenishment station is equal to $R = 2$, as seen in Fig. 9(b), it cannot be possible to recharge ABS_4 at time t_5 so that ABS_4 waits in the sleeping state until t_6 . Thus, we propose a scheduling mechanism to minimize the waiting times of ABSs for recharging under the assumption of limited number of replenishment stations as given in Alg. 4. Alg. 4 runs with the first arrival and tracks busy period of the replenishment stations ($[t_{aj}, t_{dj}]$) over the time period $[0, T]$. If there is no available station, then busy periods are computed in the case of early arrival (Lines 7-13) and accordingly, the task is updated by the control station.

As seen in Fig. 9(c), the task of ABS_3 is updated and then ABS_3 is ready for recharging at time t_3 so that ABS_4 is now scheduled after the departure of ABS_3 . Another approach could be to update the task of ABS_2 . However, in this case, we assume that $t_6 - t_4 + t_3 < t_6 - t_2 + t_1$. This is controlled in Alg. 4. Let us now discuss the computational complexity of implementing Alg. 4. Each ABS that arrives to the station for recharging executes this procedure with $O(n)$ operations. Each line between 3 to 6 is accomplished with $O(1)$ operations per discrete time step. For worst case scenario, all ABSs wait for recharging and replenishment stations are not available. The total complexity is $O(n)$ operations between Lines 8-10. Similarly, each line between 11 to 13 is accomplished

with $O(1)$ operation per discrete time step. Thus, the total complexity is $O(n^2)$ operations.

Algorithm 4 Scheduling for Recharging

```

1: Sort ABSs by arrival time over the time period  $[0, T]$  so that
    $t_{a1} \leq t_{a2} \leq \dots \leq t_{aK}$ 
2: for  $j \leftarrow 1$  to  $M'$  do
3:   if  $ABS_j$  is compatible with a station  $r$  then
4:     Schedule  $ABS_j$  to the station  $r$ 
5:      $[t_{aj}, t_{dj}] \leftarrow compute\ busy\ periods\ for\ r \in R$ 
6:      $t(r) \leftarrow t_{dj}$  // station  $r$  is busy until  $t_{dj}$ 
7:   else
8:     for  $r \leftarrow 1$  to  $R$  do
9:       new  $(t(r)_{dj}^*) = t(r)_{dj} + t(r)_{aj-1} - t(r)_{aj}$ 
10:    end for
11:    Select min(updated  $(t(r)_{dj}^*)$ )
12:    Update the task of  $ABS_j^*$ 
13:    Allocate station  $r$  at first available  $(t(r)_{dj}^*)$  and schedule
         $ABS_j$  to the defined station
14:  end if
15: end for

```

V. PERFORMANCE EVALUATION

In this section, we extensively evaluate the effectiveness of *AirNet*. To analyze this, we first consider four different schemes to deploy ABSs under the constraints of limited number of ABS: (i) Random ABS deployment (ii) ABS deployment to the locations of damaged BS (iii) Set cover approach (iv) Energy-aware ABS deployment. Then, we verify the benefits of an optimized scheduling of the ABSs' visits to the replenishment stations.

A. Simulation Setup

First, the proposed model has been implemented in MATLAB 2018a. Then, Cygwin software is used for ABS control with Software in the Loop (STIL) ArduPilot simulator [20] and MAVProxy 1.5.0 with C++ compiler.

In our simulation, we consider ABS-based communication for urban environment over 2GHz carrier frequency with $a = 4.2$ and $b = 8$ with $k_1 = 10.39$, $k_2 = 0.05$, $g_1 = 29.06$, $g_2 = 0.03$ [3]-[29]. UEs are uniformly distributed with $\lambda_u = 4 \times 10^{-2} UEs/m^2$ in 50×50 cells, where the length of each cell is 20m. We assume that ABS transmission power is $P_t = 24dBm$, battery capacity is $2 \times 10^4 mAh$, average (v_d) and maximum speed (v_{max}) are 10m/s and 20m/s, respectively. ABS transmits at power level with full speed (P_{full}) = 5W and when $v_d = 0$, $(P_s) = 0$. It is assumed that ABS weight is $(m_d) = 650g$ with $m = 4$ propellers, air density is $\rho = 1.125kg/m^3$ and charge rate current is 2.4A.

B. Benefits of Energy-Efficient Deployment

As the baseline ABS deployment comparison, Fig. 11 shows 4 different approaches with 10 ABSs as follows.

- *Random ABS deployment*: We randomly deploy ABSs to the target area with the same coverage radius ($R_{cluster} = 50m$).
- *ABS deployment to the locations of damaged BS*: We deploy the ABSs to the locations of damaged BS at fixed height ($h = 60m$).

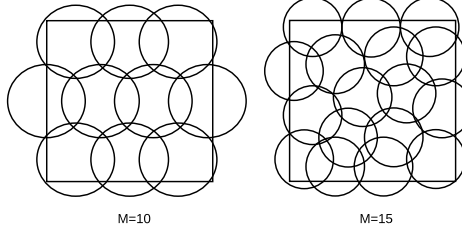


Fig. 10. Covering a given target area with $M=10$ ($R_{cluster} = 0.2182a(m)$) and $M=15$ ($R_{cluster} = 0.1796a(m)$).

- **Set cover approach:** As a baseline comparison, we analyze the study in [3]. In this scheme [3], to cover a target area, a circle packing approach is considered and then the authors compute the coverage utility and coverage radius. We made some changes in this study to apply to our scenario. First, we consider the target region as a square area instead of a circular area. Then, we focus on covering the entire target area. To exemplify this, Fig. 10 is given with 10 and 15 ABSs. As seen in the Figure, when the required number of ABSs changes, the coverage radius shows a difference. By considering this approach, we create the circles to cover all target area with the same radius ($R_{cluster} = 50m$) since [3] considers fixed circles. Then, we consider the set cover problem that selects the set with maximum number of UEs under the constraints of a limited number of the ABSs.
- **Energy-aware ABS deployment:** Our *AirNet* system that was presented in the previous section.

In Fig. 11, we set the number of ABSs as 10 and show the coverage areas for 4 schemes, respectively. First, we randomly deploy ABSs in Fig. 11(a) and analyze coverage utility for the target area. Then, in Fig. 11(b), it is assumed that terrestrial BSs are located with the distance of $200m$ in the target area and we deploy ABSs to these locations at fixed height, $h = 60m$. At each step, we select the sets which have maximum number of UEs. However, since it is not possible to cover all UEs within the coverage area of a terrestrial BSs, we deploy ABSs to maximize the covered UEs. In Fig. 11(c), we mainly focus on the prior work [3] as a baseline that uses ABSs to provide wireless coverage in a given geographical area. We initially consider covering problem with circles, $R_{cluster} = 50m$ and we define the required number of circles to cover target area as explained in [28]. Then, we focus on a set cover problem since in our scenario, we assume that the number of ABSs is limited and we select the circles in order to maximize the number of covered UEs. Finally, in Fig. 11(d), we show the proposed energy-aware ABS deployment and evaluate the results.

Fig. 12 shows the coverage utility with deployment of 10, 15, 20, and 25 ABSs. Coverage utility is the ratio of covered users to all users. We see that when the number of ABSs increases, *AirNet* provides best results, it also clearly outperforms the set cover approach. Energy-aware deployment adjusts maximum coverage area with a minimum required transmission power with Alg. 1 and enables average 24% and 3.72% increase in coverage utility when compared to the

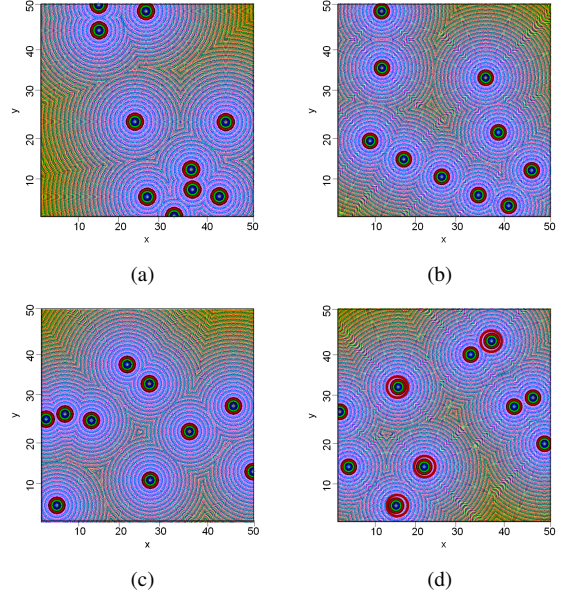


Fig. 11. ABS deployment for different schemes with 10 ABSs (a) Random ABS deployment (b) ABS deployment to the locations of damaged BS (c) Set cover approach (d) Energy-aware ABS deployment.

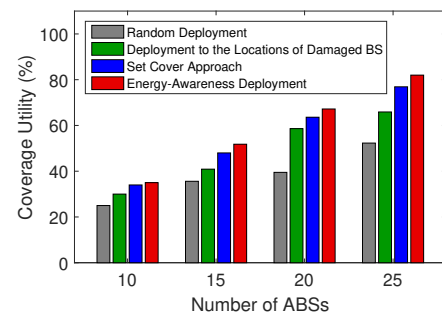


Fig. 12. Coverage utility for 4 different schemes.

random and set cover approach [3], respectively. As seen in the figure, random and deployment to the locations of damaged BS are not directly applicable for a potential solution for mission critical environments.

After energy-aware ABS deployment, we next investigate the consumed transition energy for 10 ABSs in Fig. 13. The transition energy from the control station to the designated location, $E_{trans} = \int_{t_0}^{t_1} P_{trans} dt$ and the designated location to the control station for recharging, $E_{trans} = \int_{t_2}^{t_3} P_{trans} dt$ is analyzed, where Eq. 8 gives the details. Initially, the control station was located at $(0,0)$ in the axes and ABSs are directed to the designated locations (x_j, y_j, z_j) . Then, the position of the control station is adaptively updated with Alg. 2 and we compute the consumed transition energy for individual ABSs so that the hover time is increased 8% over the Aerial Networks.

C. Demand-Aware Reconfiguration

Since user demand can vary over time in an unpredictable way, this motivates us to analyze the demands as variable and

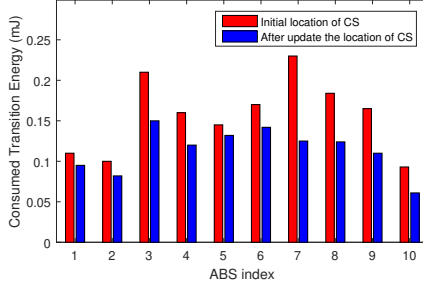


Fig. 13. Consumed transition energy of individual ABSs.

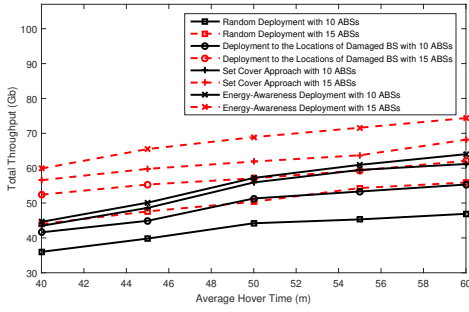


Fig. 14. Average hover time w.r.t. total throughput

also not known. Therefore, we assume that the packet arrival rate is $\lambda_i = 60$ packets/sec with Poisson distribution and the packet size distribution has a power law behavior with mean 1100 bytes to design an efficient traffic model. Power-law distribution is used to characterize the equilibrium of users' demands. Under the packet size distribution and availability of the existing resources, demand-aware reconfiguration enables to a fair resource allocation. In this respect, in Fig. 14, we show the total throughput w.r.t. average hover time with 10 and 15 ABSs. More importantly, it is shown that when the number of ABSs is increased, the proposed model enables significant improvement thanks to demand-aware reconfiguration and the rate at which the throughput does not increase the same rate for different schemes.

D. Benefits of Scheduling

Under the assumption of the limited number of replenishment stations, in order to observe the benefits of scheduling mechanism, Fig. 15 shows the normalized recharging delay before and after scheduling approaches according to different number of replenishment stations. Recharging delay is defined as the waiting time before recharging. In order to provide a clearer illustration, recharging delay is independently normalized for each different number of stations. The results are obtained with respect to the increasing number of ABSs. Note that we only focus on ABSs that wait for recharging. The benefit of providing a scheduling between ABSs and stations is clearly seen from the figure, in particular, when the number of stations increases, the results indeed outperform greatly. Thus, to obtain the results for the scheduling mechanism, we first compute the mean number of ABSs and mean charging time

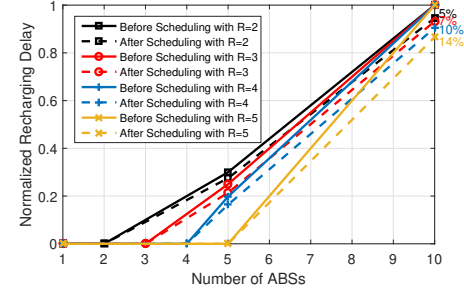


Fig. 15. Normalized recharging delay before scheduling and after scheduling with different number of replenishment station.

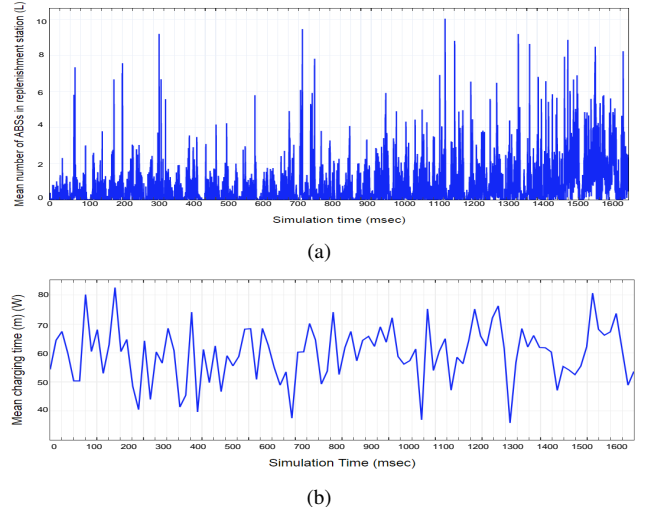


Fig. 16. (a) Mean number of ABSs and (b) Mean charging time in the replenishment station.

in the replenishment station over simulation time as shown in Figs. 16(a)-16(b) with Eqs. 25-26, respectively so that we can evaluate the recharging delay. In Fig. 16, we assume that there are 4 stations with respect to the changing number of ABSs. As expected, when the number of ABSs that needs to be recharged is higher than 4, the construction of the scheduling mechanism will be very useful to guarantee a better network management.

Next, we demonstrate the Probability Density Function (PDF) of recharging delay for 2, 3, 4 and 5 replenishment stations for one ABS in Fig. 17. Note that, in order to obtain reliable simulation estimates, we set the number of ABSs to 8. As seen in the Fig. 17, when the number of stations decreases, the probability of each ABS getting waited will increase. As the number of stations increases from 2 to 5, the value of the mean waiting time before recharging approximately drops from 3.4 to 0.94h. This implies that the increase on the number of stations will cause a significant decrease in the recharging delay and this mean value is improved with the proposed scheduling approach.

VI. CONCLUSION

This paper presented and evaluated *AirNet*, an energy-aware ABS deployment and scheduling mechanism accounting for

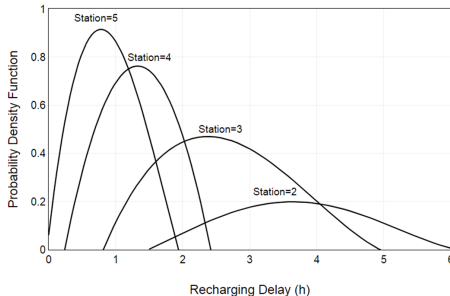


Fig. 17. Probability density function of recharging delay for one ABS. The number of replenishment station is equal to 5, 4, 3 and 2. The number of waiting ABSs is equal to 8.

replenishment stations. We addressed the problem of ABS deployment to maximize the covered UEs in an online-manner. We formulated an energy model to derive an efficient recharging strategy. Then, we presented a scheduling algorithm under the constraint a limited number of replenishment stations. Extensive simulation results demonstrate the effectiveness of the proposed algorithm in terms of the user coverage and flight endurance compared to a related work from the literature. We report on an extensive evaluation showing 24% improvement in user coverage and 8% extension in the flight endurance. We see our work as a first step and believe that it opens several interesting avenues for future research. In particular, we so far assumed a relatively simple model for the to-be-covered area, and it would be interesting to investigate more complex scenarios, e.g., due to mountains or other obstructions. It would also be interesting to consider the use of randomized algorithms.

APPENDIX A PROOF OF APPROXIMATION

In Alg. 2, we initially select M-sets that maximize the number of covered UEs. Here, OPT shows the optimal solution to maximize the covered UEs. Let us denote a_i as the number of newly covered UEs, b_i as the total number of UEs and c_i as the number of uncovered UEs at the i_{th} iteration so that $b_i = \sum_{j=1}^i a_j$ and $c_i = OPT - b_i$ [34].

The number of newly covered UEs at the $(i+1)_{th}$ iteration is equal to or greater than $1/M$ of the number of uncovered UEs after i_{th} iteration such that $a_{i+1} \geq \frac{c_i}{M}$.

Lemma: $c_{i+1} \leq (1 - \frac{1}{M})^{i+1} \cdot OPT$

Proof: By induction, we give the steps for $i = 0$.

$$\begin{aligned} c_1 &\leq (1 - \frac{1}{M}) \cdot OPT \\ OPT - b_1 &\leq OPT - OPT \cdot \frac{1}{M} \\ b_1 &\geq OPT \cdot \frac{1}{M} \\ a_1 &\geq OPT \cdot \frac{1}{M} \\ a_1 &\geq c_0 \cdot \frac{1}{M} \end{aligned} \quad (29)$$

Then, we know $a_1 \geq c_0 \frac{1}{M}$ for $i = 0$. Assume $c_i \leq (1 - \frac{1}{M})^i \cdot OPT$ is true, we show that $c_{i+1} \leq (1 - \frac{1}{M})^{i+1} \cdot OPT$ is true.

$$\begin{aligned} c_{i+1} &= c_i - a_{i+1} \\ c_{i+1} &\leq c_i - \frac{c_i}{M} \\ c_{i+1} &\leq c_i \left(\frac{1}{M} \right) \\ c_{i+1} &\leq \left(\frac{1}{M} \right)^i \cdot OPT \left(1 - \frac{1}{k} \right) \\ c_{i+1} &\leq \left(\frac{1}{M} \right)^{i+1} \cdot OPT \end{aligned} \quad (30)$$

Theorem: A greedy algorithm achieves a $(1 - \frac{1}{e})$ approximation factor.

Proof: By Lemma 1, we know that $c_M \leq (1 - \frac{1}{M})^M \cdot OPT$. Then, $(1 - \frac{1}{M})^M \approx \frac{1}{e}$ so that $c_M \leq \frac{OPT}{e}$.

$$\begin{aligned} b_M &= OPT - c_M \\ b_M &= OPT - \frac{OPT}{e} \\ b_M &= OPT \left(1 - \frac{1}{e} \right) \end{aligned} \quad (31)$$

ACKNOWLEDGEMENT

Elif Bozkaya was supported by the Scientific and Technical Research Council of Turkey (TUBITAK) Scholarship Program.

REFERENCES

- [1] <http://thoughtleadership.aonbenfield.com/Documents/20180124-ab-if-annual-companion-volume.pdf>
- [2] Cisco Visual Networking Index: Forecast and Trends, 2017-2022.
- [3] M. Mozaffari, W. Saad, M. Bennis, M. Debbah. "Efficient Deployment of Multiple Unmanned Aerial Vehicles for Optimal Wireless Coverage", IEEE Communications Letters, 20(8):1647-1650, 2016.
- [4] A. Al-Hourani, S. Kandeepan, and S. Lardner. "Optimal LAP Altitude for Maximum Coverage", IEEE Wireless Communication Letter, 3(6):569-572, 2014.
- [5] R. Yaliniz, A. El-Keyi, and H. Yanikomeroglu. "Efficient 3-D placement of an aerial base station in next generation cellular networks", in Proc. of IEEE International Conference on Communications (ICC), Kuala Lumpur, Malaysia, May 2016.
- [6] H. Ghazzai, M. B. Ghorbel, A. Kadri, J. Hossain, and H. Menouar. "Energy-Efficient Management of Unmanned Aerial Vehicles for Underlay Cognitive Radio Systems", IEEE Transactions on Green Communications and Networking, 1(4), 434-443, 2017.
- [7] J. V. Dries Hulens and T. Goedeme. "How to choose the best embedded processing platform for onboard UAV image processing", International Joint Conference Computer Vision, Imaging and Computer Graphics Theory and Applications (VISIGRAPP), Berlin, Germany, 2015.
- [8] L. Ruan, J. Wang, J. Chen, Y. Xu, Y. Yang, H. Jiang, Y. Zhang, Y. Xu. "Energy-Efficient Multi-UAV Coverage Deployment in UAV Networks: A Game-Theoretic Framework", China Communications, 194-209, October 2018.
- [9] B. Li, C. Chen, R. Zhang, H. Jiang, X. Guo. "The Energy-efficient UAV-based BS Coverage in Air-to-Ground Communications", IEEE 10th Sensor Array and Multichannel Signal Processing Workshop (SAM), 2018.
- [10] H.S. Lee, H.W. Yoo and B.H. Lee. "Deployment Method of UAVs with Energy Constraint for Multiple Tasks", IEEE Electronic Letters, 51(21), 1650-1652, 2015.
- [11] M. Alzenad, A. El-Keyi, F. Lagum, and H. Yanikomeroglu. "3D Placement of an Unmanned Aerial Vehicle Base Station (UAV-BS) for Energy-Efficient Maximal Coverage", IEEE Wireless Communications Letters, 6(4), 2017.

- [12] S. Chandrasekharan, S. Kandeepan and Robin J. Evans. "EE-CAN: Energy Efficient Clustering in Aerial Networks", IEEE 11th International Conference on Signal Processing and Communication Systems (ICSPCS), Gold Coast, QLD, Australia, 2017.
- [13] A. V. Savkin and H. Huang. "Deployment of Unmanned Aerial Vehicle Base Stations for Optimal Quality of Coverage", IEEE Wireless Communications Letter, 8(1), pp. 321-324, Feb 2019.
- [14] M. E. Mkiramweni and C. Yang. "Energy Efficiency Optimization for Wireless Unmanned Aerial Vehicle Communication Networks: A Bargaining Game Approach". 10th International Conference on Wireless Communications and Signal Processing (WCSP), Hangzhou, China, 2018.
- [15] Y. Zeng, and R. Zhang. "Energy-efficient UAV Communication with Trajectory Optimization", IEEE Transactions on Wireless Communications, 16(6), pp. 3747-376, Jun 2017.
- [16] S. Kandeepan, K. Gomez, L. Reynaud, T. Rasheed. "Aerial-Terrestrial Communications: Terrestrial Cooperation and Energy-Efficient Transmissions to Aerial Base Stations", IEEE Transactions on Aerospace and Electronic Systems, 50(4), pp.2715-2735, 2014.
- [17] A. Merwaday, A. Tuncer, A. Kumbhar, and I. Guvenc. "Improved Throughput Coverage in Natural Disasters Unmanned Aerial Base Stations for Public-Safety Communications", IEEE Vehicular Technology Magazine, pp.53-60, 2016.
- [18] M. M. Azari, F. Rosas, K. Chen, and S. Pollin. "Ultra Reliable UAV Communication Using Altitude and Cooperation Diversity", IEEE Transactions on communications, 66(1), pp.330-344, 2018.
- [19] M. Mozaffari, W. Saad, M. Bennis, and M. Debbah. "Wireless Communication Using Unmanned Aerial Vehicles (UAVs): Optimal Transport Theory for Hover Time Optimization", IEEE Transactions on Wireless communications, 16(12), pp.8052-8066, 2017.
- [20] <http://ardupilot.org/dev/docs/stl-native-on-windows.html>
- [21] A. Biniaz, P. Liu, A. Maheshwari, M. Smid. "Approximation Algorithms for the Unit Disk Cover Problem in 2D and 3D", Elsevier Computational Geometry: Theory and Applications", vol.60 pp.8–18, 2017.
- [22] D. Gross, J.F. Shortle, J.M. Thompson, C.M. Harris. "Fundamentals of Queueing Theory", Fourth Edition, A John Wiley & Sons, Inc., Publication, 2008.
- [23] M. Mozaffari, W. Saad, M. Bennis and M. Debbah. "Unmanned Aerial Vehicle with Underlaid Device-to-Device Communications: Performance and Tradeoffs" IEEE Transactions on Wireless Communications, 15(6), pp.3949-3963, 2016.
- [24] Vijay V. Vazirani "Approximation Algorithms", Springer, 2001.
- [25] X. Gao, J. Fan, F. Wu and G. Chen. "Approximation Algorithms for Sweep Coverage Problem With Multiple Mobile Sensors", IEEE/ACM Transactions on Networking, 26(2), pp.990-1003, 2018.
- [26] D'Hondt, Victor. "La representation proportionnelle des parties", 1878.
- [27] D'Hondt, Victor. "Système pratique et raisonnable de représentation proportionnelle", 1882.
- [28] K. J. Nurmela and P. R. J. Östergård. "Covering Square with up to 30 Equal Circles", Helsinki University of Technology, Laboratory for Theoretical Computer Science, 2000.
- [29] A. Al-Hourani, S. Kandeepan, and A. Jamalipour. "Modeling Air-to-Ground Path Loss for Low Altitude Platforms in Urban Environments," IEEE Global Communications Conference, Austin, TX, USA, 2014.
- [30] Z. Xiao, B. Zhu, Y. Wang, Pu Miao. "Low-Complexity Path Planning Algorithm for Unmanned Aerial Vehicles in Complicated Scenarios", IEEE Access, vol. 6: 57049-57055, 2018.
- [31] J. Tao, C. Zhong, L. Gao, H. Deng. "A Study on Path Planning of Unmanned Aerial Vehicle Based on Improved Genetic Algorithm", IEEE 8th International Conference on Intelligent Human-Machine Systems and Cybernetics, 2016.
- [32] J. L. Foo, J. Knutson, V. Kalivarapu, J. Oliver, and E. Winer. "Path Planning of Unmanned Aerial Vehicles Using B-Splines and Particle Swarm Optimization" Journal of Aerospace Computing Information and Communication 6:271-290, 2009.
- [33] M. Bekhti, M. Abdennebi, N. Achir, K. Boussetta. "Path Planning of Unmanned Aerial Vehicles With Terrestrial Wireless Network Tracking" Wireless Days 2016,Toulouse, France.
- [34] <https://www2.cs.duke.edu/courses/fall13/compsci530/notes/lec16.pdf>



Elif Bozkaya is currently PhD candidate in Department of Computer Engineering in Istanbul Technical University, Turkey and also Teaching Staff at the Department of Computer Engineering in National Defense Naval Academy, Turkey. She received her MSc degree in Computer Engineering from Istanbul Technical University, Turkey in 2015 and her BSc degree in Computer Engineering from National Defense Naval Academy, Turkey, in 2009. She was visiting researcher in Faculty of Computer Science in University of Vienna, Austria, between February-August 2019. She is the recipient of IEEE INFOCOM Best Paper Award (2018). Her research interest includes Aerial Networks, Software-Defined Networking (SDN), Vehicular Networks, Sensor Networks.



Klaus-Tycho Foerster is a PostDoc at the Faculty of Computer Science at the University of Vienna, Austria since 2018. He received his Diplomas in Mathematics (2007) & Computer Science (2011) from Braunschweig University of Technology, Germany, and his PhD degree (2016) from ETH Zurich, Switzerland, advised by Roger Wattenhofer. He spent autumn 2016 as a Visiting Researcher at Microsoft Research Redmond with Ratul Mahajan, joining Aalborg University, Denmark as a PostDoc with Stefan Schmid in 2017. His research interests revolve around algorithms and complexity in the areas of networking and distributed computing.



Stefan Schmid is a Professor at the Faculty of Computer Science, at University of Vienna, Austria. He obtained his diploma (MSc) in Computer Science at ETH Zurich in Switzerland (minor: micro/macro economics, internship: CERN) and did his PhD in the Distributed Computing Group led by Prof. Roger Wattenhofer, also at ETH Zurich. As a postdoc, he worked with Prof. Christian Scheideler at the Chair for Efficient Algorithms at the Technical University of Munich and at the Chair for Theory of Distributed Systems at the University of Paderborn, in Germany. From 2009 to 2015, Stefan Schmid was a senior research scientist at the Telekom Innovation Laboratories (T-Labs) and at TU Berlin in Germany (Internet Network Architectures group headed by Prof. Anja Feldmann). From 2015 to 2017, Stefan Schmid was a (tenured) Associate Professor in the Distributed, Embedded and Intelligent Systems group at Aalborg University, Denmark, and continued working part-time at TU Berlin, Germany. Since 2015, he serves as the Editor of the Distributed Computing Column of the Bulletin of the European Association of Theoretical Computer Science (BEATCS), since 2016 as Associate Editor of IEEE Transactions on Network and Service Management (TNSM), and since 2019 as Editor of IEEE/ACM Transactions on Networking (ToN). Stefan Schmid received the IEEE Communications Society ITC Early Career Award 2016. His research interests revolve around the fundamental and algorithmic problems of networked and distributed systems.



Berk Canberk [S'03, M'11, SM'16] is an Associate Professor at the Department of Computer Engineering in ITU. Since 2016, he has been also an Adjunct Associate Professor with the Department of Electrical and Computer Engineering at Northeastern University. He serves as an Editor in IEEE Communications Letter, IEEE Transactions in Vehicular Technology, Elsevier Computer Networks, Elsevier Computer Communications and Wiley International Journal of Communication Systems. He is the recipient of IEEE INFOCOM Best Paper Award (2018), The British Council (UK) Researcher Link Award (2017), IEEE CAMAD Best Paper Award (2016), Royal Academy of Engineering (UK) NEWTON Research Collaboration Award (2015), IEEE INFOCOM Best Poster Paper Award (2015), ITU Successful Faculty Member Award (2015) and Turkish Telecom Collaborative Research Award (2013). His current research areas include Software-Defined Networking (SDN) and Network Function Virtualization (NFV) in 5G Systems, and Next Generation Network Management Systems.